

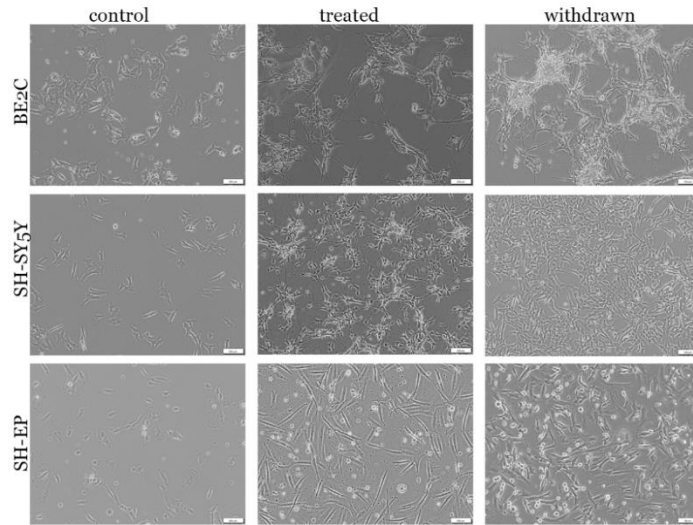
Supplementary Material

Supplementary Movie S1: Time-lapse movie showing BE2C cells maintaining the differentiated phenotype after withdrawal of ATRA.

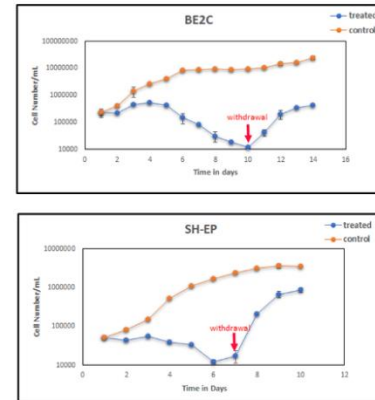
Supplementary Movie S2: Time-lapse movie showing SH-SY5Y cells reverting after withdrawal of ATRA

Supplementary Figure S1

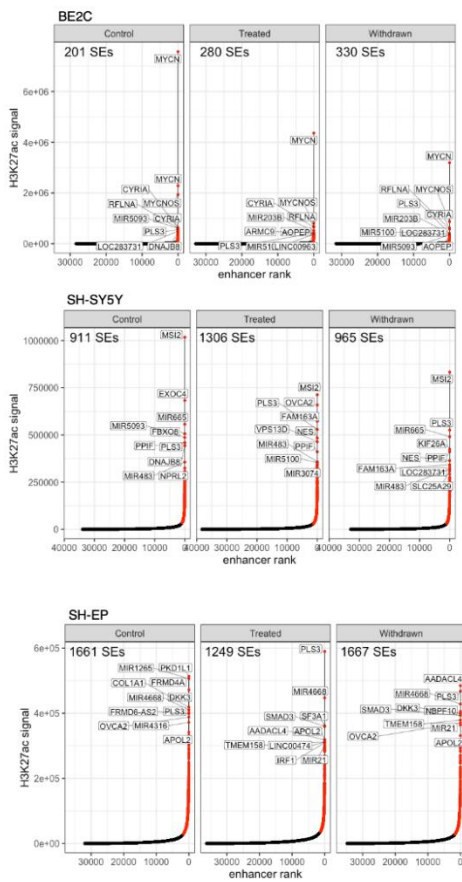
A



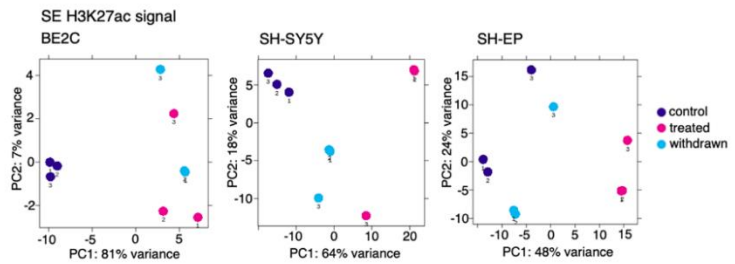
B



C

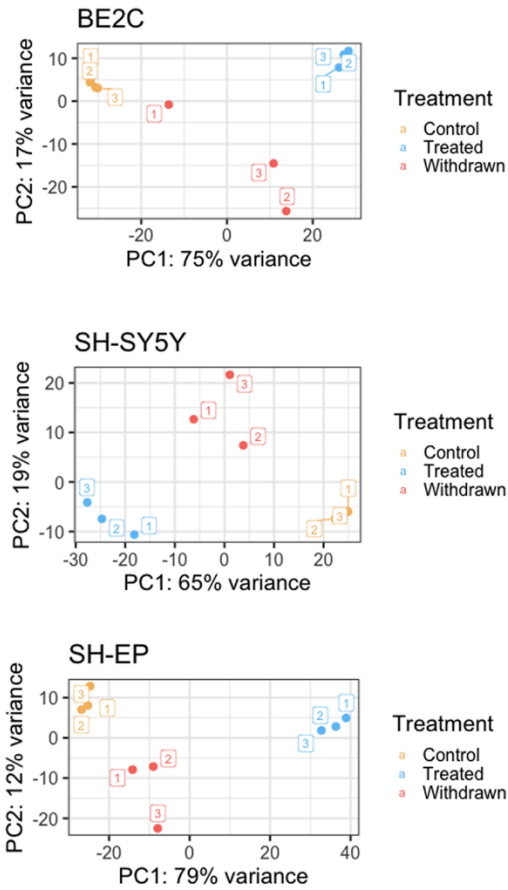


D

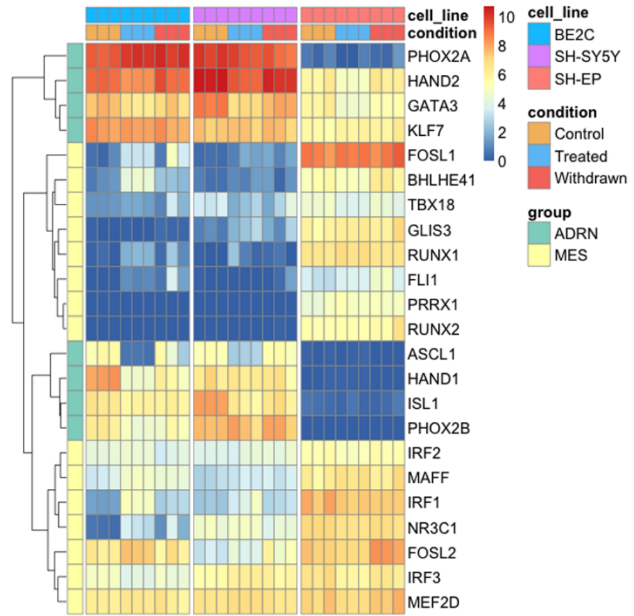


Supplementary Figure S2

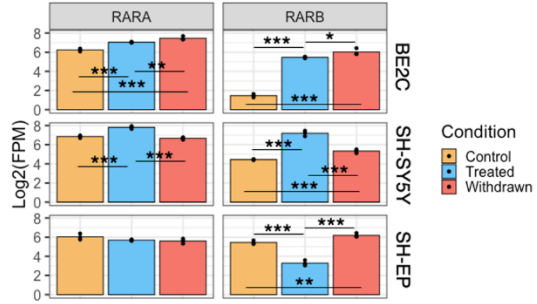
A



B

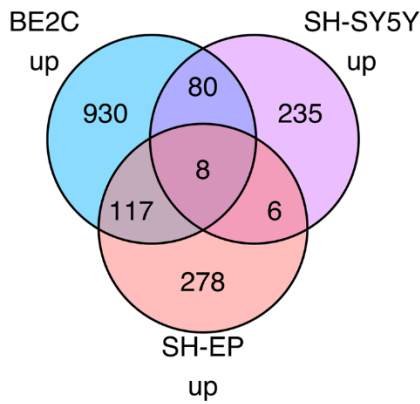


C



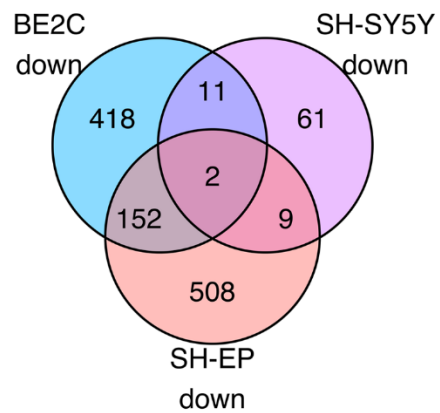
D

ATRA upregulated genes

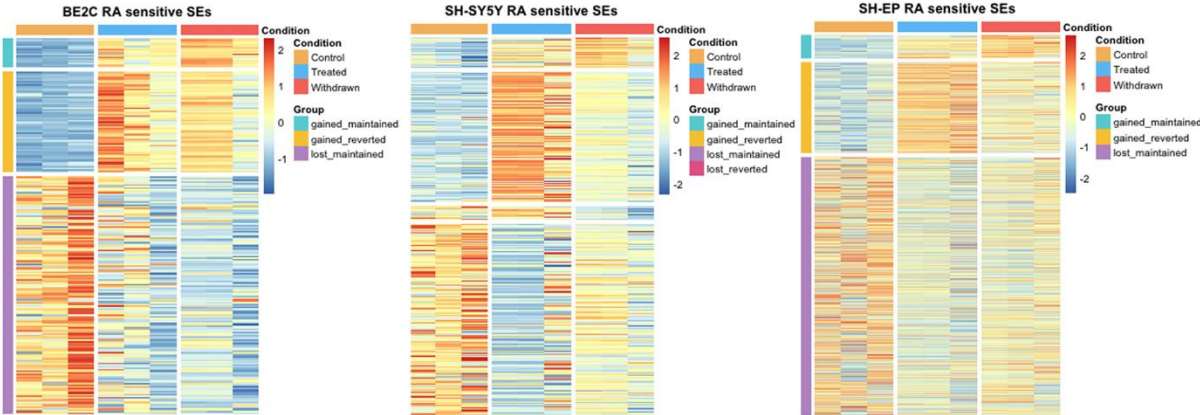


E

ATRA downregulated genes

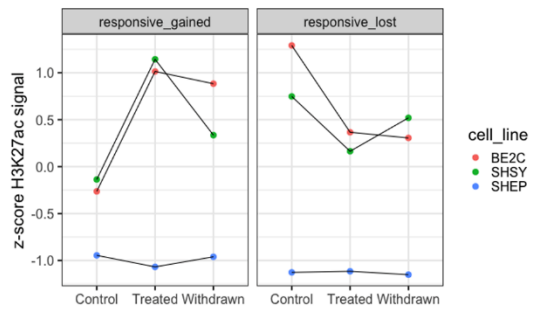


Supplementary Figure S3

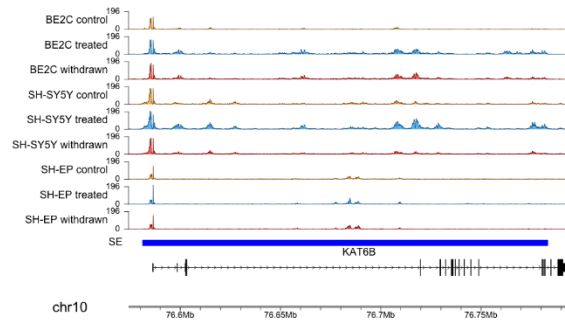


Supplementary Figure S4

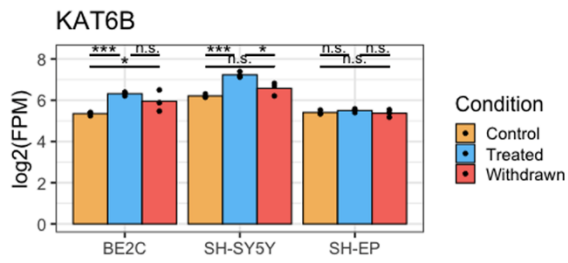
A



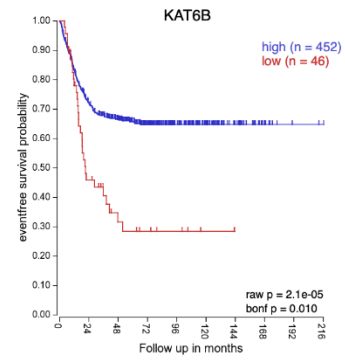
B



C

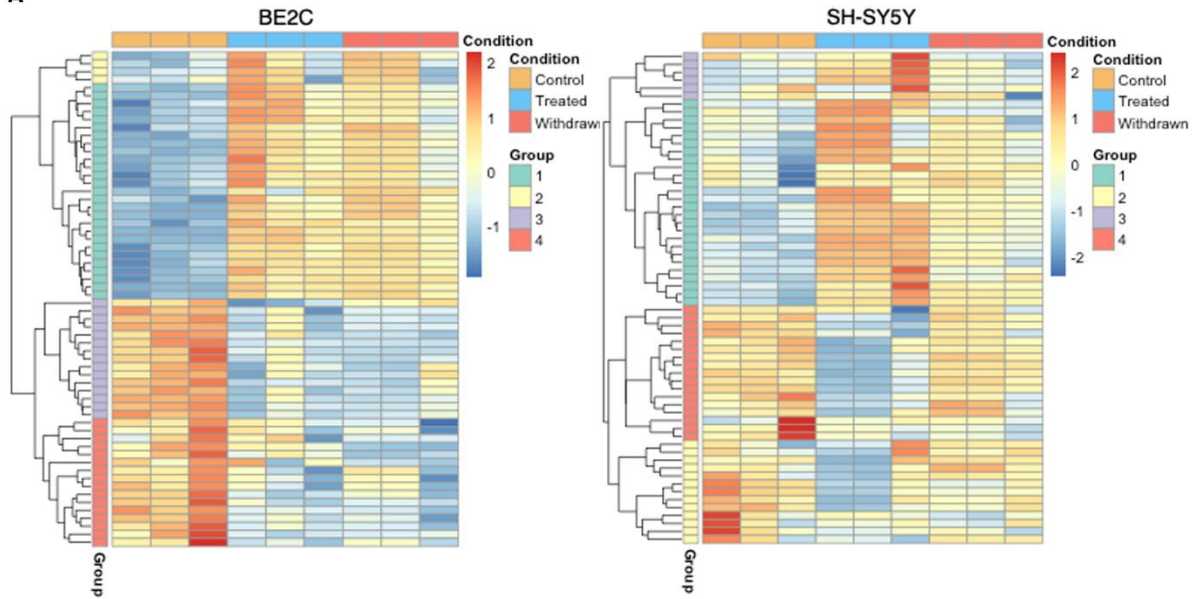


D

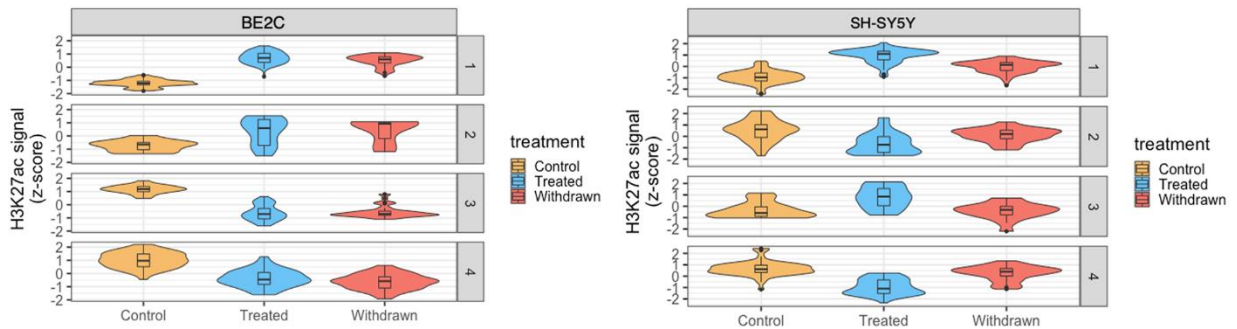


Supplementary figure S5

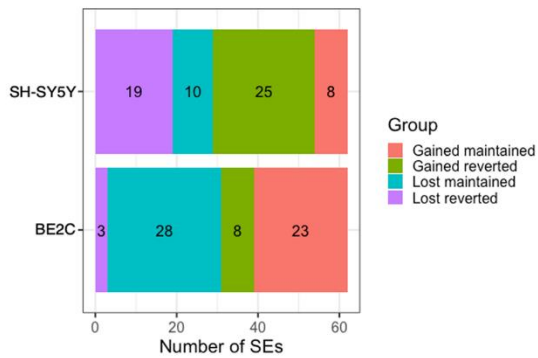
A



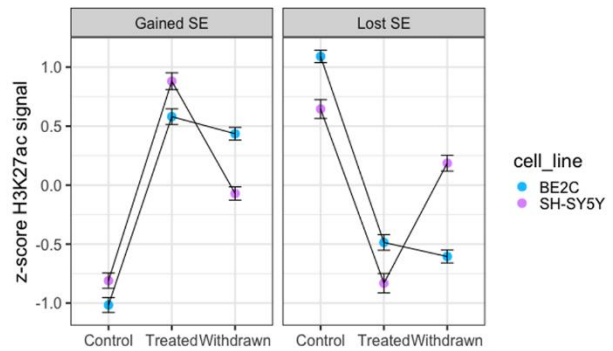
B



C

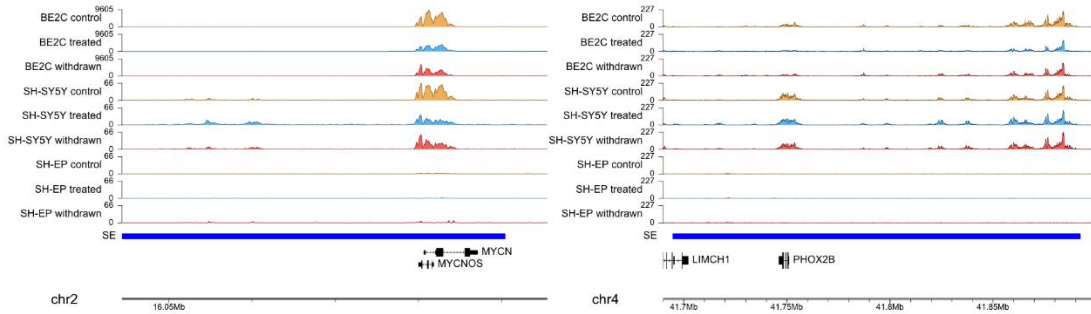


D

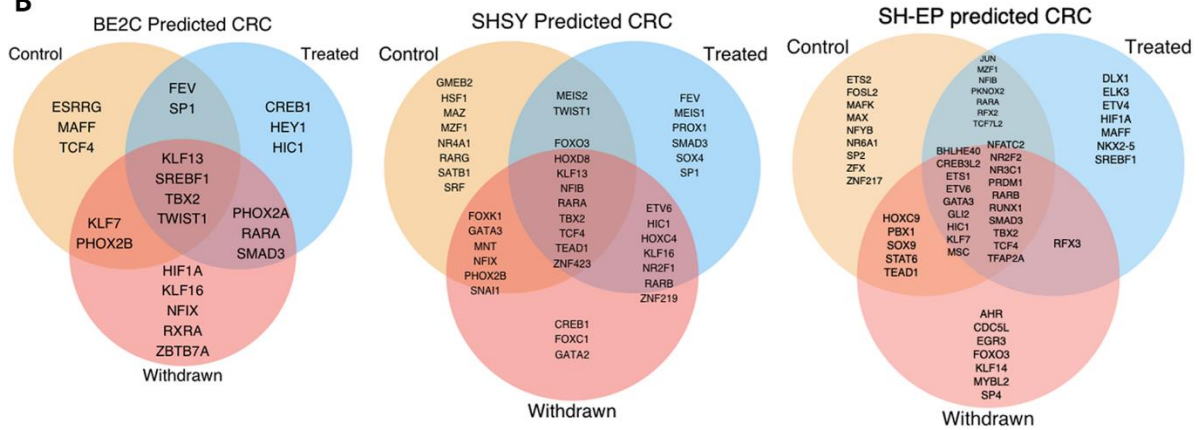


Supplementary Figure S6

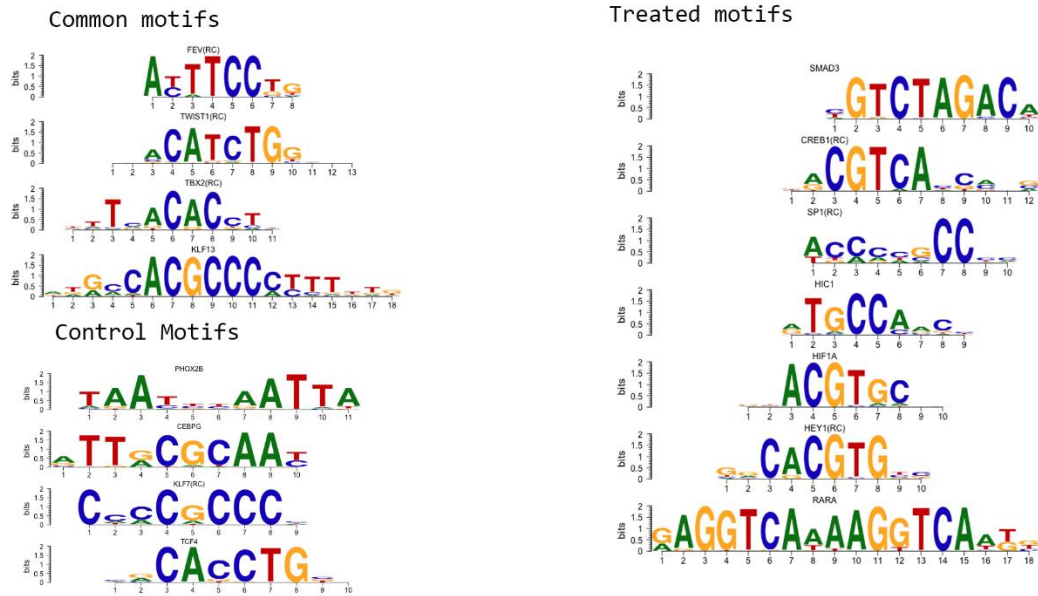
A



B

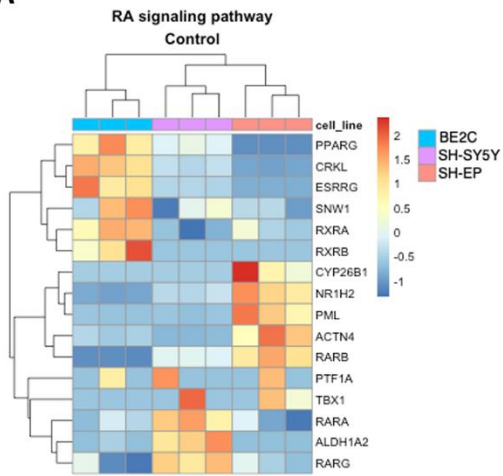


C

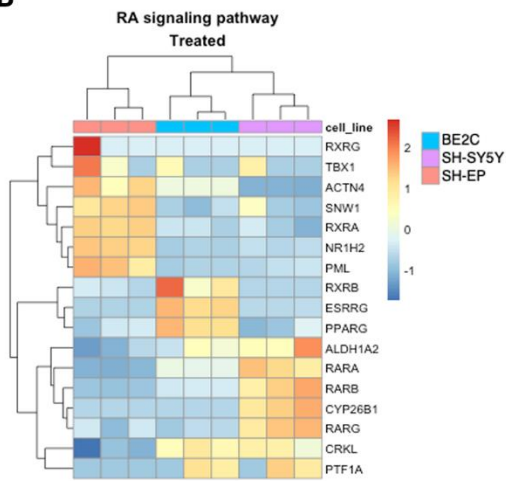


Supplementary Figure S7

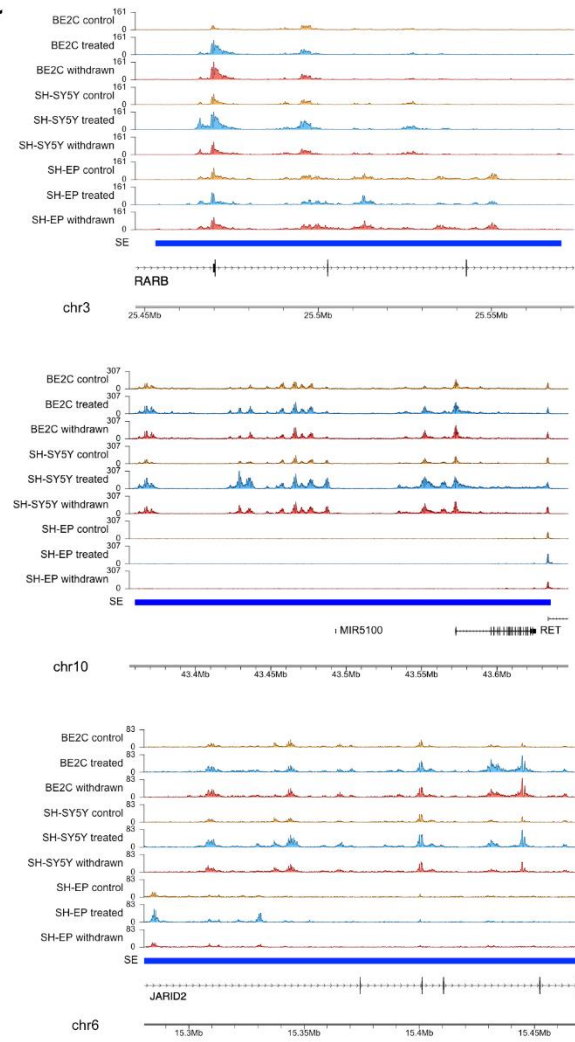
A



B



C



Supplementary Figure Legends

Supplementary figure S1: (A) Phase contrast microscopy images of responsive cell lines (BE2C, SH-SY5Y) and resistant cell line (SH-EP) under control, upon ATRA treatment and subsequent removal of ATRA. Scale bar indicates 100 μ M (except for 'SH-EP withdrawn' which is 50 μ M). (B) Growth curve of responsive (BE2C) and resistant (SH-EP) cell lines grown in 24-well plate. Each value is the average of cell counts from 2 wells, taken at an interval of 24 hours. Time point of withdrawal is marked in red arrow. (C) Ranked enhancer plots, showing H3K27ac signal at enhancers and super-enhancers in BE2C, SH-SY5Y and SH-EP under each condition identified using ROSE. Regions designated as super-enhancers highlighted in red, the top 10 super-enhancers from each condition are annotated with their predicted target gene. (D) PCA of H3K27ac signal at super-enhancer regions identified by ROSE in control, treated, or withdrawn conditions for each cell line.

Supplementary figure S2: (A) PCA of RNA-seq data in each condition, for each cell line. (B) Heat map showing expression of *ADRN* and *MES* markers in the 3 different cell lines after ATRA treatment and withdrawal. (C) Bar plots showing the expression of *RARA* and *RARB* in control, treated and withdrawn conditions in responsive cell lines (BE2C and SH-SY5Y) and resistant cell line (SH-EP). Adjusted p-value displayed; Statistical significance determined using DESeq2 (* $p_{adj} < 0.05$, ** $p_{adj} < 0.01$, *** $p_{adj} < 0.001$). Venn diagram shows genes significantly upregulated (D) and downregulated (E) after ATRA treatment in each cell line ($p_{adj} < 0.05$, $\log_2FC > 2$).

Supplementary figure S3: Heatmap showing normalised H3K27ac signal (z-score) at ATRA responsive super-enhancers identified in BE2C, SH-SY5Y and SH-EP, and grouped by patterns of H3K27ac change.

Supplementary figure S4: (A) Average change in H3K27ac signal at gained or lost super-enhancers in responsive (BE2C and SH-SY5Y) and resistant cell lines (SH-EP). Y-axis shows z-score average expression for each group of super-enhancers. (B) Representative ChIP-seq tracks displaying super-enhancer regions of *KAT6B* identified in ATRA responsive cell lines. (C) Bar plot showing the expression of *KAT6B* in control, treated and withdrawn conditions in responsive cell lines (BE2C and SH-SY5Y) and resistant cell line (SH-EP). Statistical significance determined using DESeq2 (* $p_{adj} < 0.05$, ** $p_{adj} < 0.01$, *** $p_{adj} < 0.001$). (D) Kaplan-Meier survival curves showing the probability of event free survival in two groups of neuroblastoma patients, split based on their tumor expression level of *KAT6B*.

Supplementary figure S5: (A) Heatmap showing changes in H3K27ac levels at super-enhancers which gain or lose H3K27ac in response to ATRA treatment in BE2C and SH-SY5Y cell lines. Data is z-scaled for each super-enhancer region, within each cell line. Data was split into 4 groups for each cell line by hierarchical clustering, based on the pattern of H3K27ac after ATRA treatment and withdrawal (B) Violin plots summarizing the H3K27ac signal data shown in Supplementary Figure 5A. (C) Bar chart showing the number of super-enhancers in each of the four groups identified in the violin plot in each cell line (SH-SY5Y and BE2C). (D) Average change in H3K27ac

signal at gained or lost super-enhancers shown in Figure S5A in BE2C and SH-SY5Y. Y-axis shows z-score H3K27ac for each group of SEs.

Supplementary figure S6: (A) Representative ChIP-seq tracks displaying super-enhancers associated with *MYCN* (left panel) and *PHOX2B* (right panel). (B) Venn diagram showing the predicted CRC TFs of each cell line under control, treated and ATRA withdrawn conditions. (C) Binding motifs of the predicted CRCs unique to control and treated conditions and those which are common to both conditions.

Supplementary figure S7: Heatmaps showing the change in expression of retinoic acid signaling pathway genes in (A) control and (B) treated conditions, z-scaled by row. (C) Representative ChIP-seq tracks displaying super-enhancers associated with RARB (upper panel), RET (middle panel) and JARID2 (lower panel).